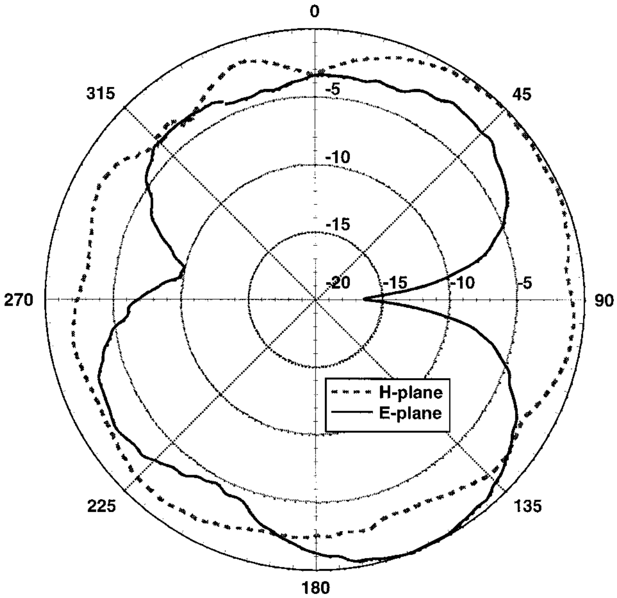

Figure 3 Measured *E*- and *H*-plane copolar radiation patterns

impedance nature of the array is governed by the location of the shorting pins and the feed network.

REFERENCES

1. R.C. Johnson and H. Jasik, Antenna engineering handbook, McGraw-Hill, New York, 1984, 2nd ed., chap. 7.
2. J.R. James and P.S. Hall, Handbook of microstrip antennas, Peter Peregrinus, London, England, 1989, vol. 2, chap. 20.
3. D.I. Wu, Omnidirectional circularly-polarized conformal microstrip array for telemetry applications, Proc IEEE Antennas Propagat Symp, June 1995, pp. 998–1001.
4. R.B. Waterhouse, Small microstrip patch antenna, Electron Lett 31 (1995), 604–605.
5. K.-L. Wong and Y.-F. Lin, Small broadband rectangular microstrip antenna with chip-resistor loading, Electron Lett (1997), 1593–1594.
6. R.B. Waterhouse, S.D. Targonski, and D.M. Kokotoff, Design and performance of small printed antennas, IEEE Trans Antennas Propagat 46 (1998), 1629–1633.
7. Rogers Corporation, http:/www.rogers-corp.com/mwu/litinbl.htm (fabrication information).

A SIMPLE ALGORITHM FOR ACCURATE LOCATION OF LEAKY-WAVE POLES FOR GROUNDED INHOMOGENEOUS DIELECTRIC SLABS

Vincenzo Galdi[1] and Innocenzo M. Pinto[1]
[1] The Waves Group, D.I.I.I.E.
University of Salerno
I-84084 Fisciano (SA), Italy
and
[1] Faculty of Engineering
University of Sannio at Benevento
I-82100 Benevento, Italy

Received 2 August 1999

ABSTRACT: *A rigorous framework and an efficient numerical implementation for computing leaky-wave poles for grounded inhomogeneous dielectric (multi-) layers are presented. The pertinent transverse-resonance (eigenvalue) equations, obtained by power-series solution of the related Sturm–Liouville problems, are solved by means of a Padé-approximant-based root-finding procedure. Numerical simulations show that very accurate results (ten decimal figures, on average) are usually obtained with a mild computational and programming effort, over a reasonably wide spectral range.* © 2000 John Wiley & Sons, Inc. Microwave Opt Technol Lett 24: 135–140, 2000.

Key words: *leaky-wave modes; inhomogeneous dielectric slabs; Padé approximants*

I. INTRODUCTION

The widespread use of dielectric (multi-) layers in many microwave and millimeter-wave applications (e.g., as substrates for printed transmission lines and antennas), as well as in modern optical devices (e.g., couplers, filters, modulators) motivated a considerable effort, during the last two decades, for a deeper understanding of wave-propagation phenomena in such structures, and more accurate and computationally less expensive numerical techniques for their analysis.

In this connection, *leaky-wave* modes [1–3] often play a key role both in describing the underlying physics and in providing efficient representation tools. As is well known [1–3], leaky-wave modes, although being (discrete) solutions of the same eigenvalue problem as the guided modes, do *not* satisfy a regularity-at-infinity (typical of guided modes) nor the radiation boundary conditions. Actually, they exhibit a *complex* propagation constant with a large imaginary part, and their field amplitudes grow transversely and decay axially. Hence, they do *not* represent physical solutions, although they could be interpreted as guided modes propagating below the cutoff point [3]. However, despite their *unphysical* character, there are several applications where (a finite number of) leaky-wave modes can be fruitfully exploited to represent the continuous radiation spectrum, with a considerable model simplification [4]. For instance, information on the location of leaky-wave eigenvalues in the complex plane is crucial for a judicious choice of a deformed integration path in the Sommerfeld integrals typically arising when computing the electromagnetic radiation from a dipole in the presence of a slab [1, 2]. In these applications, leaky-wave eigenvalues arise as complex poles of the integrand function, and it has been shown that, for moderate slab thicknesses and/or observation points relatively close to the slab, when applying the steepest descent (or the saddle-point) method of integration [1, 2], some of these poles (at a reasonable distance from the saddle point) need to be captured in order to obtain accurate results [1, 2, 5]. Furthermore, in several applications (e.g., leaky-wave antennas, printed-circuit lines, etc.), knowledge of the dominant leaky-wave modes often gives an immediate and useful insight into the radiation/leakage phenomena, and sometimes provides effective design hints.

The location of leaky-wave poles for (un)grounded *homogeneous* dielectric slabs has been extensively investigated in the past, and a number of analytical approximations (see, e.g., [3, 6]) as well as numerical procedures (see, e.g., [7]) have been proposed. On the other hand, *inhomogeneous* dielectric (multi-) layers, widely used in optical waveguides and components, are becoming popular in microwave and millimeter-wave devices as well [8]. In addition, (piecewise) continuously varying permittivity profiles are potentially useful models of, e.g., moist soils in subsurface radar applications. Most available numerical techniques for computing leaky-wave poles for inhomogeneous slabs (see, e.g., [9, 10] and references therein for a thorough review) are based on the transfer-matrix approach (for deriving the eigenvalue equations) and various root-finding algorithms, and usually require considerable computational and programming effort.

In this paper, we introduce a simple and systematic approach which allows an accurate location of leaky-wave poles with mild computational and programming effort. The proposed approach relies upon a rigorous derivation of the relevant eigenvalue equations through a power-series solution of the Sturm–Liouville problems ruling the field components in the slab, coupled to an efficient Padé-approximant-based, *exponentially* converging root-finding algorithm in the complex plane. The needed initial guesses are estimated through a *bootstrapping* strategy based on the low-frequency approximations proposed in [6] and linear extrapolation.

The remainder of the paper is organized as follows. In Section II, the derivation of the relevant transverse-resonance equations (henceforth TREs) is outlined. In Section III, the root-finding strategy is described. In Section IV, some numerical examples involving single as well as multilayer slabs are presented in order to assess the accuracy of the proposed approach, and to show its capabilities. Conclusions follow under Section V. An implicit $\exp(i\omega t)$ time-harmonic dependence is assumed and suppressed throughout the paper.

II. DERIVATION OF THE TRANSVERSE-RESONANCE EQUATIONS

An inhomogeneous dielectric layer backed by a perfect conducting plane is considered, as depicted in Figure 1. The permittivity profile is written as follows [11]:

$$\epsilon_r(x) = \epsilon_r^{(0)}[1 - 2\Delta f(x)], \qquad \Delta = \frac{\epsilon_r^{(0)} - \epsilon_r^{(d)}}{2\epsilon_r^{(0)}}, \qquad f(0) = 0, \qquad f(d) = 1 \tag{1}$$

where the profile function $f(x)$ is assumed to be analytic and monotonic within the interval $0 \le x \le d$, d being the layer thickness. Furthermore, we assume the slab as lossless, and $\epsilon_r^{(0)} > \epsilon_r^{(d)}$. As is well known, such a structure supports a finite number of transverse electric (henceforth TE) and transverse magnetic (henceforth TM) modes that (except for the dominant ones) exhibit a cutoff frequency above which they propagate as bound surface waves (guided modes). Below the cutoff frequency, they become *improper* [3], and the longitudinal propagation constant may assume complex values (leaky modes) [1–3].

Because of the homogeneity and the infinite extent of the structure along the y, z-directions, the problem is actually one dimensional. Accordingly, the fields can be assumed as independent on the y-variable, whereas their z-dependence can be written as $\exp(-ik_z z)$, k_z being the longitudinal propagation constant. This dependence henceforth will be suppressed for notational simplicity. On the other hand, the x-dependence of the tangential field components in the slab is ruled by the well-known following equations [11]:

TE modes:

$$\begin{cases} \left[\dfrac{\partial^2}{\partial x^2} + k_0^2\epsilon_r^{(0)}\mu_r - k_z^2 - [\epsilon_r^{(0)} - \epsilon_r^{(d)}]\,\mu_r k_0^2 f(x)\right] \\ \quad \times E_y(k_z, x) = 0 & (2) \\ E_y(k_z, 0) = 0 & (3) \\ H_z(k_z, x) = -\dfrac{i}{k_0\eta_0\,\mu_r}\,\dfrac{\partial E_y(k_z, x)}{\partial x} & (4) \end{cases}$$

TM modes:

$$\begin{cases} \left[\dfrac{\partial^2}{\partial x^2} - \dfrac{1}{\epsilon_r(x)}\dfrac{d\epsilon_r(x)}{dx}\dfrac{\partial}{\partial x} + k_0^2\epsilon_r^{(0)}\mu_r - k_z^2 \right. \\ \quad \left. - [\epsilon_r^{(0)} - \epsilon_r^{(d)}]\,\mu_r k_0^2 f(x)\right] H_y(k_z, x) = 0 & (5) \\ E_z(k_z, x) = \dfrac{i\eta_0}{k_0\epsilon_r(x)}\,\dfrac{\partial H_y(k_z, x)}{\partial x} & (6) \\ E_z(k_z, 0) = 0 & (7) \end{cases}$$

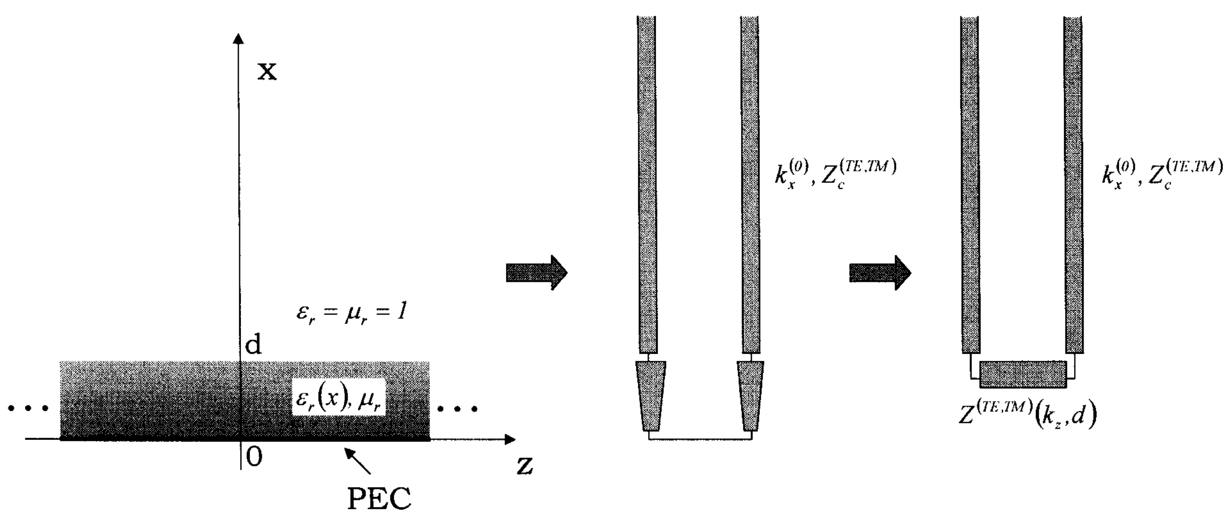

Figure 1 Problem geometry and equivalent transmission lines

where $k_0 = 2\pi/\lambda_0$ and η_0 denote, respectively, the free-space wavenumber and the characteristic impedance, and μ_r is the (constant) relative permeability.

The eigenvalue equations, whose complex roots give the sought leaky-wave poles, can be derived by enforcing the transverse-resonance condition [1–3] in the corresponding equivalent (nonuniform) transmission lines (see Fig. 1), viz.

$$Z^{(\mathrm{TE})}(k_z, d) + Z_c^{(\mathrm{TE})} = Z^{(\mathrm{TE})}(k_z, d) + \frac{k_0\eta_0}{k_x^{(0)}} = 0 \quad (8)$$

$$Z^{(\mathrm{TM})}(k_z, d) - Z_c^{(\mathrm{TM})} = Z^{(\mathrm{TM})}(k_z, d) - \frac{k_x^{(0)}\eta_0}{k_0} = 0 \quad (9)$$

where $k_x^{(0)} = (k_0^2 - k_z^2)^{1/2}$. The needed impedances at the interface with free space, $Z^{(\mathrm{TE})}(k_z, d)$, $Z^{(\mathrm{TM})}(k_z, d)$, can be computed by solving the pertinent Riccati equations [1, 2, 12] or, equivalently, Eqs. (2)–(7), since

$$Z^{(\mathrm{TE})}(k_z, d) = \frac{E_y(k_z, d)}{H_z(k_z, d)} = ik_0\eta_0\,\mu_r \frac{E_y(k_z, d)}{\dfrac{\partial E_y(k_z, d)}{\partial x}} \quad (10)$$

$$Z^{(\mathrm{TM})}(k_z, d) = \frac{E_z(k_z, d)}{H_y(k_z, d)} = i\frac{\eta_0}{k_0\epsilon_r^{(d)}H_y(k_z, d)}\frac{\partial H_y(k_z, d)}{\partial x}. \quad (11)$$

As by assumption $f(x)$ is analytic and $\epsilon_r(x)$ does not vanish in $[0, d]$, the Sturm–Liouville problems (2), (5) admit a convergent power series solutions in $0 \le x \le d$ [12, 13].

By enforcing the McLaurin expansions,

$$f(x) = \sum_{n=1}^{\infty} f_n(k_0x)^n, \qquad E_y(k_z, x) = \sum_{n=0}^{\infty} a_n(k_0x)^2 \quad (12)$$

$$\frac{1}{\epsilon_r(x)}\frac{d\epsilon_r(x)}{dx} = k_0\sum_{n=0}^{\infty} g_n(k_0x)^n,$$

$$H_y(k_z, x) = \sum_{n=0}^{\infty} b_n(k_0x)^n \quad (13)$$

into (2), (5), differentiating term by term, and equating to zero all coefficients of the resulting power series in k_0x, a recursive relation for the unknown coefficients a_n, b_n is readily found [12, 13]:

$$a_n = \frac{[\epsilon_r^{(0)} - \epsilon_r^{(d)}]\,\mu_r \sum_{j=1}^{n-2} f_j a_{n-j-2} - \left[\epsilon_r^{(0)}\mu_r - \dfrac{k_z^2}{k_0^2}\right]a_{n-2}}{n(n-1)}, \quad n \ge 2 \quad (14)$$

$$b_n = \frac{[\epsilon_r^{(0)} - \epsilon_r^{(d)}]\,\mu_r \sum_{j=1}^{n-2} f_j b_{n-j-2} + \sum_{j=0}^{n-1}(n-j-1)g_j b_{n-j-1} - \left[\epsilon_r^{(0)}\mu_r - \dfrac{k_z^2}{k_0^2}\right]b_{n-2}}{n(n-1)}, \quad n \ge 2. \quad (15)$$

It is easily understood that, our interest being in computing the impedances (10), (11), the coefficients a_1, b_0 can be chosen arbitrarily, whereas from the boundary conditions (3), (7) at the ground plane, it follows that

$$a_0 = b_1 = 0. \quad (16)$$

Accordingly, the sought impedances at the interface with free-space are

$$Z^{(\mathrm{TE})}(k_z, d) = i\eta_0\,\mu_r \frac{\sum_{n=0}^{\infty} a_n(k_0d)^n}{\sum_{n=1}^{\infty} na_n(k_0d)^{n-1}} \quad (17)$$

$$Z^{(\mathrm{TM})}(k_z, d) = i\frac{\eta_0}{\epsilon_r^{(d)}}\frac{\sum_{n=1}^{\infty} nb_n(k_0d)^{n-1}}{\sum_{n=0}^{\infty} b_n(k_0d)^n}. \quad (18)$$

It could be worth pointing out that the above procedure can be extended to handle ungrounded and/or multilayer configurations as well. This requires a rather straightforward iteration of the above procedure, where each layer is terminated by an impedance accounting for the loading effect of possible upstream layers. In this more general case, the impedances describing the effect of possible further layers for $x < 0$ (see Fig. 1), say $Z^{(\mathrm{TE})}(k_z, 0)$, $Z^{(\mathrm{TM})}(k_z, 0)$, determine the values of the coefficients a_0, b_1. Hence, instead of (16), we use

$$a_0 = -i\frac{Z^{(\mathrm{TE})}(k_z, 0)a_1}{\eta_0\,\mu_r},$$

$$b_1 = -i\frac{Z^{(\mathrm{TM})}(k_z, 0)\epsilon_r^{(0)}b_0}{\eta_0}. \quad (19)$$

III. ROOT-FINDING PROCEDURE

In this section, we focus on the numerical computation of the complex roots of the TREs (8), (9), which yield the sought leaky-wave poles.

Standard root-finding methods are usually based on locally linear (e.g., Newton–Raphson [14]) or quadratic (e.g., Muller [15]) approximations of the complex function under analysis, and their success strongly depends on a good choice of the initial guesses. More robust algorithms (e.g., Davidenko [16]) are also available, but their implementation is generally more involved, and a full explicit expression of the complex function is usually required.

In this paper, we adopt a different strategy, described in [17], which relies on a local rational (type II Padé) approximation [12, 17]. The complex function $F(k_z)$, whose roots need to be computed, is initially evaluated at three points (initial guesses), $k_z^{(1)}$, $k_z^{(2)}$, $k_z^{(3)}$. By exploiting these three samples, a Padé (rational) approximant of type II [11, 15] can be unambiguously determined via point matching. The zero of the obtained Padé approximant, say $k_z^{(4)}$, is used together with the points $k_z^{(2)}$, $k_z^{(3)}$ to evolve the procedure at the next step, where another Padé approximant is determined, and so on. Therefore, given three initial guesses $k_z^{(1)}$, $k_z^{(2)}$, $k_z^{(3)}$, the procedure generates a sequence $\{k_z^{(i)}\}$ of approximations, from which the estimated root at the ith iteration is [17]

$$k_z^{(i)} = \frac{k_z^{(i-1)}\dfrac{(k_z^{(i-2)}-k_z^{(i-3)})}{F(k_z^{(i-1)})} + k_z^{(i-2)}\dfrac{(k_z^{(i-3)}-k_z^{(i-1)})}{F(k_z^{(i-2)})} + k_z^{(i-3)}\dfrac{(k_z^{(i-1)}-k_z^{(i-2)})}{F(k_z^{(i-3)})}}{\dfrac{(k_z^{(i-2)}-k_z^{(i-3)})}{F(k_z^{(i-1)})} + \dfrac{(k_z^{(i-3)}-k_z^{(i-1)})}{F(k_z^{(i-2)})} + \dfrac{(k_z^{(i-1)}-k_z^{(i-2)})}{F(k_z^{(i-3)})}}, \qquad i > 3. \quad (20)$$

It is readily understood that each iteration requires one function evaluation only, and therefore the computational burden is the same as the Newton–Raphson and Muller methods. Furthermore, it can be shown [17] that the above procedure exhibits an *exponential* convergence, provided the initial guesses are not too far away from the sought root.

A rather simple and inexpensive strategy to obtain reasonably good initial guesses is to exploit the low-frequency approximations for the sought complex poles $k_z = \beta - i\alpha$, proposed by Guglielmi and Jackson [6] for grounded homogeneous slabs:

TE_m modes:

$$\begin{cases} \beta_m d \approx q + \dfrac{q}{q-1}(p - q + \log q) \\ \alpha_m d \approx \dfrac{q}{q-1}(m-1)\pi, \qquad m = 1, 2, \ldots \end{cases} \quad (21)$$

TM_m modes:

$$\begin{cases} \beta_m d \approx \log\sqrt{\dfrac{\epsilon_r \mu_r + 1}{\epsilon_r \mu_r - 1}} \\ \alpha_m d \approx \dfrac{\pi}{2}(2m-1), \qquad m = 1, 2, \ldots \end{cases} \quad (22)$$

where m is the modal index, d is the slab thickness, ϵ_r, μ_r are, respectively, the relative electric permittivity and magnetic permeability, and

$$q = p + \frac{p}{p-1}\log p, \qquad p = \log\left(\frac{2}{k_0 d\sqrt{\varepsilon_r \mu_r - 1}}\right). \quad (23)$$

IV. NUMERICAL RESULTS

The convergence features of the proposed root-finding strategy have been first investigated for the simplest case of a homogeneous slab, for which closed-form dispersion equations are available, and are illustrated in Figure 2. This preliminary simulation has been carried out using the arbitrary-precision functions provided by MATHEMATICA™ [17] and, owing to the logarithmic scale used, it allows us to appreciate the exponential convergence of the proposed procedure, and its better performance as compared to Muller's method (exponentially convergent as well). As is well known [3], the TE_1-mode holds a real propagation constant even in its improper range, and thus it can be analyzed using standard real root-finding schemes. Therefore, we considered the TE_2-mode, and used as initial guesses the low-frequency approximation (21) plus its $\pm 1\%$ variations, which differ roughly by some 30% from the exact root.[1] The number of accurate figures reported in Figure 2 has been estimated as the number of invariant (stable) decimal figures between two successive iterations,[2] i.e.,

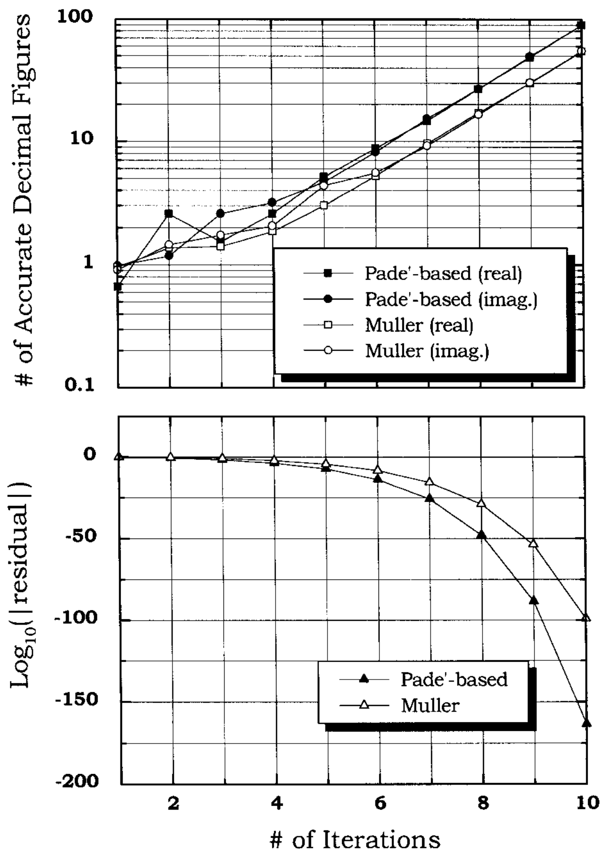

Figure 2 Homogeneous slab. Convergence features of Padé-based and Muller's root-finding algorithms for TE_2 leaky mode ($\epsilon_r = 3$, $\mu_r = 1$, $k_0 d = 0.25$)

$$N_{\text{figures}}^{(\text{real})} = -\log_{10}\left|\frac{\mathrm{Re}[k_z^{(i)}] - \mathrm{Re}[k_z^{(i-1)}]}{\mathrm{Re}[k_z^{(i)}]}\right|,$$

$$N_{\text{figures}}^{(\text{imag.})} = -\log_{10}\left|\frac{\mathrm{Im}[k_z^{(i)}] - \mathrm{Im}[k_z^{(i-1)}]}{\mathrm{Im}[k_z^{(i)}]}\right| \quad (24)$$

whereas the *residual* indicates the value of the left-hand side of the TRE (8) at the estimated root. It is observed that, even though the initial guess was not really close to the exact root, a modest number of iterations is required for achieving very accurate results (e.g., six iterations for a ten-figure accuracy). The better performance of the proposed procedure as compared to Muller's can be justified by taking into account the very nature of the complex function under analysis, which contains pole singularities, and hence turns out to be better locally approximated by a rational function than by a quadratic one.

[1] Different variations also have been employed, without a sensible change in the convergency rate.

[2] After a short transient, this actually coincides with the number of accurate figures, provided the method converges.

The proposed root-finding algorithm has been applied in conjunction with the TRE derivation presented in Section II to compute the leaky-wave poles for an inhomogeneous slab described by the following quadratic profile:

$$f(x) = a\frac{x}{d} + (1-a)\left(\frac{x}{d}\right)^2, \qquad 0 < x < d, 0 \le a \le 1. \quad (25)$$

The algorithm has been implemented using the standard (double precision) accuracy of a PC desktop workstation, using the low-frequency approximations (21), (22) applied to an *effective* homogeneous dielectric slab with relative electric permittivity $\epsilon_r^{(0)}$ to estimate the initial guesses. Table 1 shows the number of iterations required by the iterative root-finding algorithm to provide the eight-figure targeted accuracy[3] for various TE- and TM-modes. Again, the TE_1-mode was not considered, its propagation constant holding real values in the improper range. As expected, it is observed that, as the frequency is raised, the root-finding procedure is prone to fail (i.e., convergence is not reached within a given number of iterations or the estimated root pertains to a different modal index) since the initial guesses provided by the low-frequency approximations (21), (22) become too far from the exact roots.

A simple way to overcome this limitation, and to compute the dispersion laws over a wider spectral range, is to employ a *bootstrapping* strategy, i.e., using *first* at low frequencies (e.g., $k_0 b < 10^{-3}$) the Guglielmi–Jackson approximations (21), (22), and *then* exploiting the already computed lower frequency values to (e.g., linearly) extrapolate quite *trustworthy* initial guesses for the higher frequencies. When applied to the above quadratic profile, this strategy allows us to cover a considerably wider spectral range, as shown in Figure 3. In these simulations, two low-frequency estimations ($k_0 b =$ 0.001, 0.002) and linear extrapolation are used to analyze the spectral range $0.01 < k_0 b < 4$. An average number of four iterations per frequency point (frequency step = 0.02) was found to be sufficient to achieve a ten-figure average accuracy.

As a final example, we consider a grounded two-layer slab composed of an exponential profile and a quadratic one:

$$\epsilon_r(x) = \begin{cases} \epsilon_r^{(0)}[1 - 2\Delta_1 f_1(x)], & 0 < x < d_1 \\ \epsilon_r^{(d_1)}[1 - 2\Delta_2 f_2(x)], & d_1 < x < d_2 \end{cases} \quad (26)$$

[3] Obviously, the targeted accuracy on the sought leaky-wave poles dictates the truncation criteria for the power series in (17), (18).

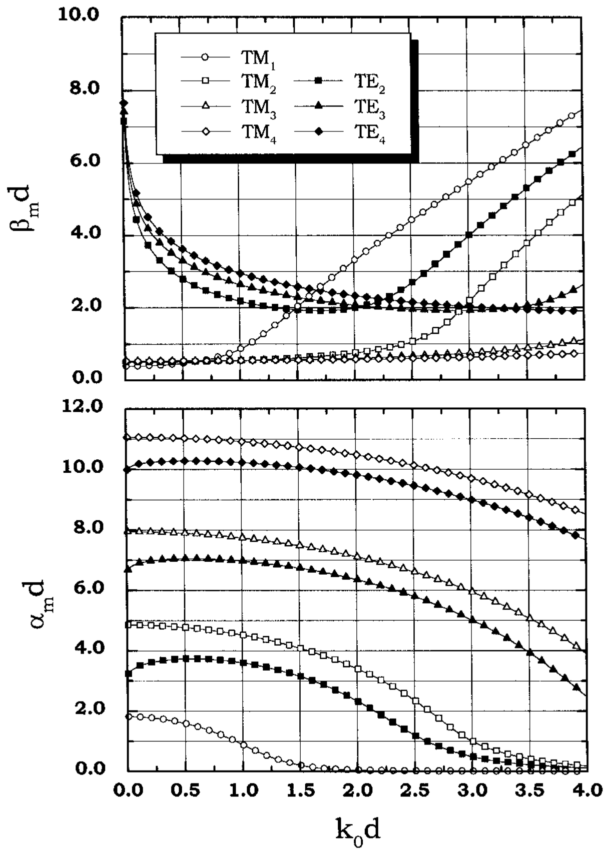

Figure 3 Quadratic-profile slab. Dispersion diagrams for the first seven leaky modes [$\epsilon_r^{(0)} = 4$, $\epsilon_r^{(d)} = 2$, $\mu_r = 1$, $a = 0.3$ in Eq. (25)]

$$\Delta_1 = \frac{\epsilon_r^{(0)} - \epsilon_r^{(d_1)}}{2\epsilon_r^{(0)}}, \qquad \Delta_2 = \frac{\epsilon_r^{(d_1)} - \epsilon_r^{(d_2)}}{2\epsilon_r^{(d_1)}} \quad (27)$$

$$f_1(x) = \frac{1 - \exp(x/d_1)}{1 - e}, \qquad 0 < x < d_1 \quad (28)$$

$$f_2(x) = a\frac{x - d_1}{d_2 - d_1} + (1-a)\left(\frac{x - d_1}{d_2 - d_1}\right)^2, \qquad d_1 < x < d_2, 0 \le a \le 1. \quad (29)$$

Results are reported in Figure 4 in the form of dispersion diagrams for various TE- and TM-modes. The same bootstrapping strategy as the previous example has been used,

TABLE 1 Quadratic-Profile Slab; Number of Iterations Needed by the Padé-Based Root-Finding Algorithm for the First Seven Leaky Modes [$\epsilon_r^{(0)} = 4$, $\epsilon_r^{(d)} = 2$, $\mu_r = 1$, $a = 0.3$ in Eq. (25)]

$k_0 d$	TE_2	TE_3	TE_4	TM_1	TM_2	TM_3	TM_4
0.0001	5	6	6	6	5	5	5
0.0005	5	6	7	6	5	5	5
0.001	6	6	7	6	5	5	5
0.005	6	6	8	6	5	5	5
0.01	6	7	9	6	5	5	5
0.05	6	9	failure	6	5	5	5
0.1	7	failure	—	5	5	5	5
0.5	failure	—	—	5	5	5	5
1	—	—	—	6	5	5	5
2	—	—	—	failure	7	6	6
3	—	—	—	—	failure	11	8

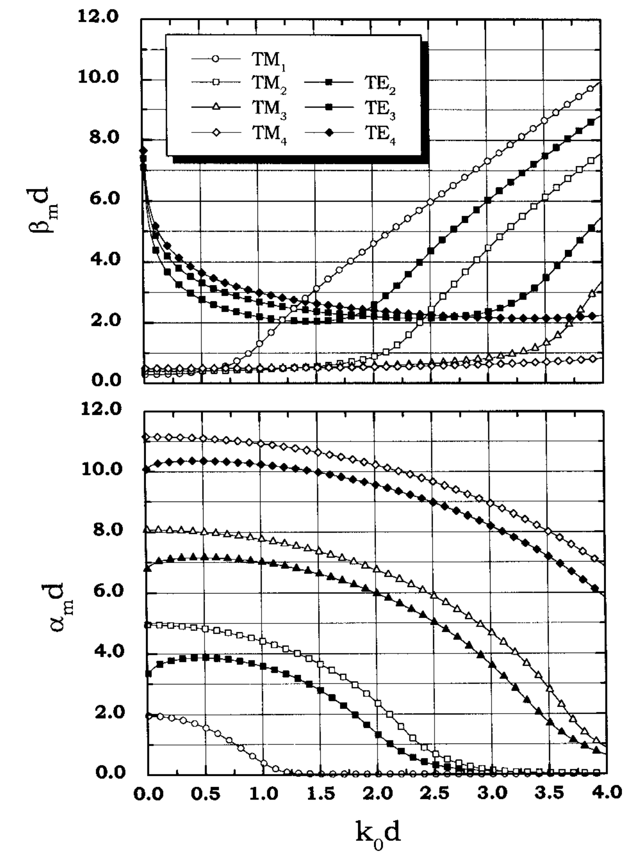

Figure 4 Two-layer slab. Dispersion diagrams for the first seven leaky modes [$\epsilon_r^{(0)} = 7$, $\epsilon_r^{(d_1)} = 5$, $\epsilon_r^{(d_2)} = 2$, $\mu_r = 1$, $a = 0.1$, $d_1 = d_2 = 0.5d$ in Eqs. (26)–(29)]

and the convergence and accuracy features were found to be essentially the same.

V. CONCLUSIONS

A simple algorithm that allows an inexpensive and accurate computation of leaky-wave poles for grounded inhomogeneous dielectric slabs has been presented. The proposed method relies on a rigorous derivation of the relevant TREs, which are solved using an efficient Padé-approximant-based root-finding procedure in the complex plane. Numerical simulations, involving single- and two-layer profiles, show that the proposed method is attractive in terms of accuracy, computational budget, and implementation ease.

Worthwhile extensions, presently under investigation, involve (bi)anisotropic layers and cylindrical geometries.

REFERENCES

1. L.B. Felsen and N. Marcuvitz, Radiation and scattering of waves, Prentice Hall, Englewood Cliffs, NJ, 1973.
2. R.E. Collin, Field theory of guided waves, IEEE Press, Piscataway, NJ, 1992, 2nd ed.
3. D. Marcuse, Theory of dielectric optical waveguides, Academic, New York, 1974.
4. N. Marcuvitz, On field representation in terms of leaky modes, IRE Trans Antennas Propagat AP-4 (1956), 192–194.
5. D.P. Nyquist, Leaky-wave and radiation modes of the planar dielectric waveguide—A review of their origin and significance, Proc 16th URSI Int Symp Electromag Theory, Thessaloniki, Greece, May 1998, pp. 488–490.
6. M. Guglielmi and D.R. Jackson, Low-frequency location of the leaky-wave poles for a dielectric layer, IEEE Trans Microwave Theory Tech 38 (1990), 1743–1746.
7. C.-I.G. Hsu, R.F. Harrington, J.R. Mautz, and T.K. Sarkar, On the location of leaky wave poles for a grounded dielectric slab, IEEE Trans Antennas Propagat 39 (1991), 346–349.
8. X. Jiang and K. Wu, Analysis of unbounded circuits and antennas considering finite extent and inhomogeneous dielectric, Proc 1997 IEEE-MTT Int Microwave Symp, Denver, CO, June 1997, pp. 617–620.
9. E. Anemogiannis, E.N. Glytsis, and T.K. Gaylord, Efficient solution of eigenvalue equations of optical waveguiding systems, J Lightwave Technol 12 (1994), 2080–2084.
10. E. Anemogiannis, E.N. Glytsis, and T.K. Gaylord, Determination of guided and leaky modes in lossless and lossy planar multilayer optical waveguides: Reflection pole method and wavevector density method, J Lightwave Technol 17 (1999), 929–941.
11. A.W. Snyder and J.D. Love, Optical waveguide theory, Chapman & Hall, London, England, 1983.
12. C.M. Bender and S.A. Orszag, Advanced mathematical methods for scientists and engineers, McGraw-Hill, New York, 1978.
13. V. Galdi and I.M. Pinto, Higher-order impedance boundary conditions for metal-backed inhomogeneous dielectric layers, Microwave Opt Technol Lett 22 (1999), 249–254.
14. R.L. Johnston, Numerical methods: A software approach, Wiley, New York, 1982.
15. D.E. Muller, A method for solving algebraic equations using an automatic computer, Math Tables, Aids of Comput 10 (1956), 208–215.
16. H.A.N. Hejase, On the use of Davidenko's method in complex root search, IEEE Trans Microwave Theory Tech 41 (1993), 141–143.
17. V.I. Kukulin, V.M. Krasnopol'sky, and J. Horácek, Theory of resonances. Principles and applications, Academia, Praha, 1989.
18. S. Wolfram, The Mathematica book, Wolfram Media/Cambridge University Press, New York, 1996, 3rd ed.

CONTROL OF THE GAIN–FREQUENCY RESPONSE OF A VANE-LOADED GYRO-TWT BY BEAM AND MAGNETIC FIELD PARAMETERS

G. Singh,[1] P. V. Bhaskar,[1] S. M. S. Ravi Chandra,[1] P. K. Jain,[1] and B. N. Basu,[1]
[1] Centre of Research in Microwave Tubes
Department of Electronics Engineering
Institute of Technology
Banaras Hindu University
Varanasi 221005, India

Received 27 July 1999

ABSTRACT: *The cold dispersion relation of a vane-loaded cylindrical waveguide was combined with the hot dispersion relation of a gyro-TWT in an unloaded waveguide to obtain the hot dispersion relation of a vane-loaded gyro-TWT. Both the device gain and bandwidth were increased by controlling the beam parameters, namely, the voltage, current, and velocity pitch factor of the beam, as well as its location. The device gain and bandwidth characteristics were also found to be highly sensitive to the background magnetic field. Study clearly demonstrated the need to take into account the role of the beam and background magnetic field parameters in efforts to broadband a gyro-TWT by using innovative structures like a vane-loaded cylindrical waveguide.* © 2000 John Wiley & Sons, Inc. Microwave Opt Technol Lett 24: 140–145, 2000.